ADVANCED MATERIALS
www.advmat.de

Ionic Liquid Interface as a Cell Scaffold

Takeshi Ueki, Koichiro Uto, Shota Yamamoto, Ryota Tamate, Yuji Kamiyama, Xiaofang Jia, Hidenori Noguchi, Kosuke Minami, Katsuhiko Ariga, Hongxin Wang, and Jun Nakanishi**

In sharp contrast to conventional solid/hydrogel platforms, water-immiscible liquids, such as perfluorocarbons and silicones, allow the adhesion of mammalian cells via protein nanolayers (PNLs) formed at the interface. However, fluorocarbons and silicones, which are typically used for liquid cell culture, possess only narrow ranges of physicochemical parameters and have not allowed for a wide variety of cell culturing environments. In this paper, it is proposed that water-immiscible ionic liquids (ILs) are a new family of liquid substrates with tunable physicochemical properties and high solvation capabilities. Tetraalkylphosphonium-based ILs are identified as non-cytotoxic ILs, whereon human mesenchymal stem cells are successfully cultured. By reducing the cation charge distribution, or ionicity, via alkyl chain elongation, the interface allows cell spreading with matured focal contacts. High-speed atomic force microscopy observations of the PNL formation process suggest that the cation charge distribution significantly altered the protein adsorption dynamics, which are associated with the degree of protein denaturation and the PNL mechanics. Moreover, by exploiting dissolution capability of ILs, an ion-gel cell scaffold is fabricated. This enables to further identify the significant contribution of bulk subphase mechanics to cellular mechanosensing in liquid-based culture scaffolds.

1. Introduction

Mammalian cells are mostly cultured in plastic dishes or chemically cross-linked hydrogels that do not normally relax the stress derived from cell contractility. This is because cells apply physical forces to the substrate and need to obtain sufficient mechanical feedback (stress or strain) for their survival.[1] Moreover, mesenchymal stem cells utilize this mechanical information to determine their own lineage of differentiation, among neurons, muscles, and osteoblasts, depending on the substrate elasticity. Rather surprisingly, cells can adhere and spread on the interfaces between water and water-immiscible liquids, such as fluorocarbons.[2] Hence, cells can engage mechanosensing machinery even at the liquid | liquid interface. From a practical viewpoint, cell culture on a deformable liquid scaffold may lead to emulsion 3D bioreactors with high culturing efficiency.[2c,3] The cell adhesion at the fluid interfaces is

T. Ueki, K. Uto, S. Yamamoto, R. Tamate, Y. Kamiyama, K. Minami, H. Wang, J. Nakanishi
Research Center for Macromolecules & Biomaterials
National Institute for Materials Science (NIMS)
1-1 Namiki, Tsukuba, Ibaraki 305-0044, Japan
E-mail: ueki.takeshi@nims.go.jp; nakanishi.jun@nims.go.jp

T. Ueki, Y. Kamiyama, H. Noguchi
Graduate School of Life Science
Hokkaido University
Kita 10, Nishi 8, Kita-ku Sapporo 060-0810, Japan

X. Jia[+], K. Ariga
Research Center for Materials Nanoarchitectonics (MANA)
National Institute for Materials Science (NIMS)
1-1 Namiki, Tsukuba, Ibaraki 305-0044, Japan

H. Noguchi
Research Center for Energy and Environmental Materials (GREEN)
National Institute for Materials Science (NIMS)
1-1 Namiki, Tsukuba, Ibaraki 305-0044, Japan

K. Ariga
Department of Advanced Materials Science
Graduate School of Frontier Sciences
The University of Tokyo
5-1-5 Kashiwa-no-ha, Chiba 277-0882, Japan

J. Nakanishi
Graduate School of Advanced Science and Engineering
Waseda University
3-4-1 Okubo, Tokyo, Shinjuku-ku 169-8555, Japan

J. Nakanishi
Graduate School of Advanced Engineering
Tokyo University of Science
6-3-1 Niijuku, Tokyo, Katsushika-ku 125-8585, Japan

The ORCID identification number(s) for the author(s) of this article can be found under https://doi.org/10.1002/adma.202310105

[+]Present address: School of Pharmaceutical Sciences (Shenzhen), Shenzhen Campus of Sun Yat-sen University, Shenzhen 518107, China

DOI: 10.1002/adma.202310105

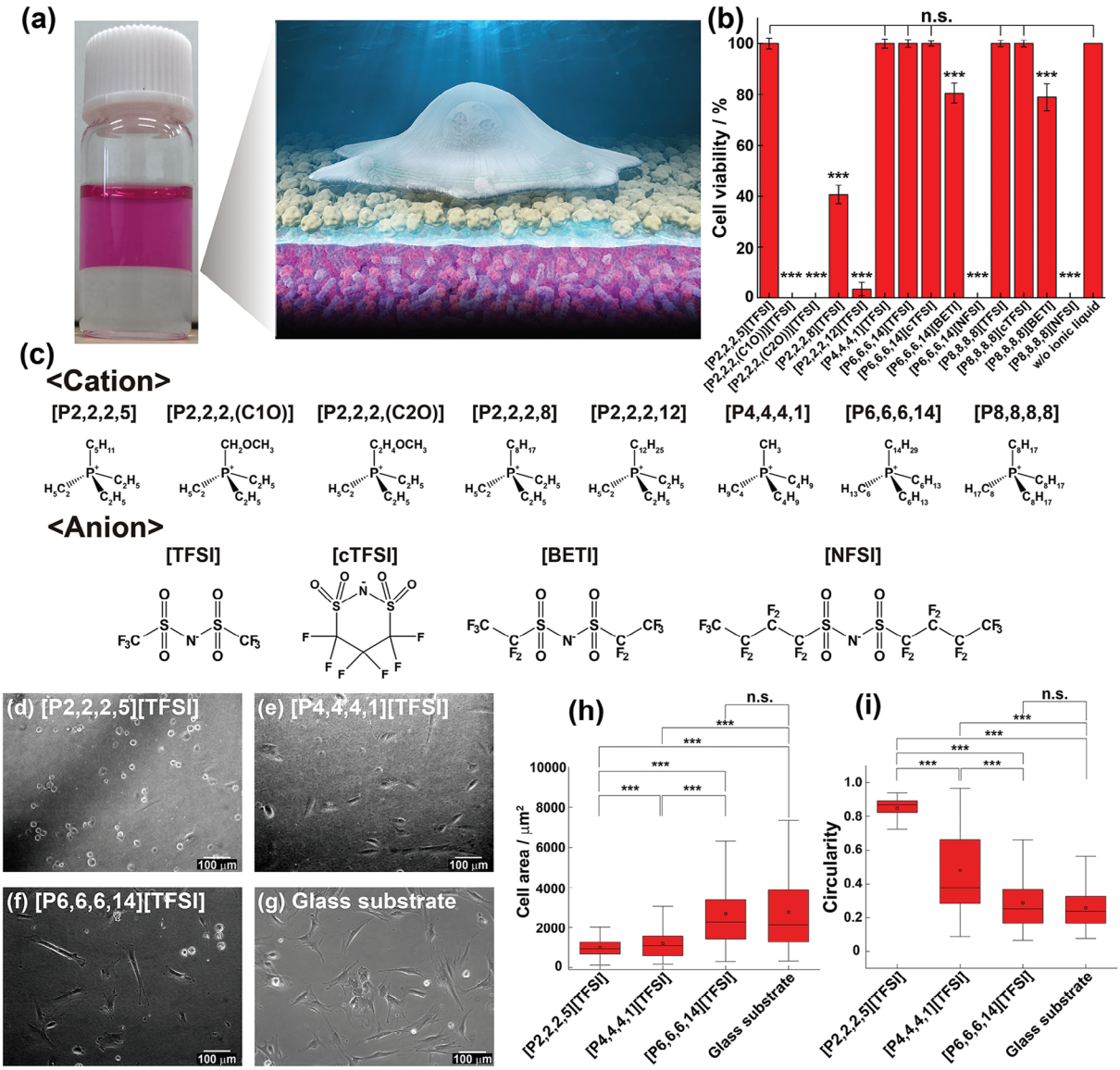

Figure 1. a) A photograph and image of cell culture at a hydrophobic ionic liquid (IL) and culture medium interfaces. b) hMSCs viability cultured at glass substrate in the presence of phosphonium IL cultured after 24 h. The cell viability was estimated by dividing the total live cell area in the presence and absence of ILs. c) Chemical structure of alkylphosphonium cation and hydrophobic sulfonylimide anion appeared in (b). Microscopic observation of human mesenchymal stem cells (hMSCs) at d) [P2,2,2,5][TFSI], e) [P4,4,4, 1][TFSI], f) [P6,6,6,14][TFSI], and g) glass substrate interfaces cultured after 24 h. Scale bars represent 100 μm. h) Cell area and i) circularity of hMSCs at IL interfaces and glass substrate as control after 24 h from cell seeding. *** $P < 0.05$ (Student's *t*-test).

mediated by the culture medium-derived jammed protein nanolayers (PNLs) formed at the interface, which are robust enough to sustain cellular traction forces.[4] Previously, we successfully manipulate the fate of human mesenchymal stem cells (hMSCs) to differentiate into the neuronal lineage or maintain the undifferentiated state by appropriately selecting the hydrophobic liquids and/or molecules to be adsorbed at the interface.[5] To further expand the differentiation spectrum of the hMSCs using liquid-based substrates for tissue engineering and therapeutic applications, it is straightforward to broaden the range of physicochemical properties of hydrophobic liquids because the mechanical strength of PNLs is highly dependent on interfacial tension and polarity.[6] However, there are only limited choices of hydrophobic liquids, such as fluorocarbons and silicones, since most exert severe cytotoxicity and are lighter than water. In addition, cells can sense the mechanical properties of their underneath at a depth of more than 65 μm from the interface.[7] Therefore, cellular fate can be determined not only by the mechanical properties of the PNL at the interface but also by the bulk mechanics.

In view of this situation, we herein developed a liquid interface culturing technology using a hydrophobic ionic liquid (IL) as a substrate (**Figure 1**a). ILs are often called "designer solvents" because there is an infinite number of possible chemical

structures and combinations of ions for IL components.[8] Therefore, by customizing the structure of ILs, the ranges of their physicochemical parameters, including polarity, viscosity, surface tension, and ionicity, can be greatly expanded compared with those of conventional liquids.[9] Moreover, unlike fluorocarbons, ILs can dissolve various substrates,[10] which is suitable for changing the bulk mechanics of the hydrophobic phases, as well. In this study, we sought ILs with negligible cytotoxicity and found that alkylphosphonium-type ILs are promising candidates. By taking advantage of the designer nature of ILs, we manipulated the van der Waals interactions of the constituted ions of ILs and the charge distribution of cations to investigate their effects on PNL formation and cell adhesion. High-speed atomic force microscopy (AFM) allowed us to visualize single-molecule protein dynamics upon adsorption at the IL interfaces and highlighted the significant differences in their kinetics depending on the cation structures. Furthermore, by utilizing the good solvent capability of ILs, we fabricated an ion gel,[11] in which a polymer network is swollen by an IL, and demonstrated the controllability of bulk mechanics and interfaces, both of which influence cell adhesion behavior.

2. Results and Discussion

First, the cytotoxicity of ILs was examined. Although there are many reports on cell cytotoxicity, dose-dependency of their pharmacological efficacy such as EC_{50} and IC_{50} is often used. Since the ILs used in this study should be water-immiscible to form liquid | liquid interface, such dose-dependent cytotoxicity is not useful. Therefore, we used LIVE/DEAD analysis to estimate the cytotoxicity of typical hydrophobic onium ILs (Figure S1, Supporting Information). Briefly, the cell viability ratio was estimated for the cells cultured at glass substrate in the presence of a droplet of each hydrophobic IL. Note that the ammonium-based ILs resulted in cell death within 24 h, whereas the some phosphonium-based ILs exhibit less or no cytotoxicity in any of the mammalian cell lines tested, that is, hMSCs, HeLa (human cell line derived from cervical cancer), MDCK (canine kidney epithelial), and A549 (human cell line derived from lung cancer) (Figures S2–S6, and S9–S14 Supporting Information) and Figure 1b,c highlight the results of cytotoxicity and chemical structure of alkyl-phosphonium ILs used in this study. A detailed discussion of the results of cytotoxicity tests can be found in the Supporting Information. Among the low-cytotoxic phosphonium ILs, we selected three representative ILs for the following study, namely [P2,2,2,5][TFSI], [P4,4,4,1][TFSI], and [P6,6,6,14][TFSI]. These ILs exhibit different levels of cation charge distribution, or ionicity, depending on the length of alkyl chain lengths.[12] More specifically, [P2,2,2,5][TFSI] possessing relatively short alkyl chains is categorized a "good IL" exhibiting more ion-dissociated, while [P6,6,6,14][TFSI] possessing long alkyl group is categorized a "poor IL" exhibiting more ion-paired or ion-associated and is close to molecular liquids.[12,13] We expected that the difference significantly impacts the protein adsorption behaviors at the IL interfaces similarly to that observed on the different crystal planes of solid ionic crystals,[14] and eventually altering cell adhesion behaviors. Furthermore, in addition to ionicity, which is a property specific to ILs, typical polarity parameters vary depending on the structure of the ILs. Table S1 (Supporting Information) summarizes the polarity parameters of the typical ILs, molecular liquids, and fluorocarbons. Unlike fluorocarbons, the polarity of ILs ranges from 2-propanol and water in terms of $E_T(30)$, which is a typical indicator of solvent polarity.[15] We have examined how the liquid properties of ILs, which can vary widely in liquid parameters specific to these ILs and also common to molecular liquids, affect the cellular behavior at the liquid interface. In addition, ILs are generally thermally, (electro)chemically stable. In particular, the sulfonylimide anions selected for this study are highly resistant to hydrolysis and will not decompose in water even when used for long-term culture.[8,9]

With this set of ILs, we demonstrated the cell-spreading behaviors of hMSCs at the water-IL interfaces. (Figure 1d–f) Most cells exhibited spherical morphologies at the [P2,2,2,5][TFSI] interface, with only a few cells spreading. Conversely, at the [P6,6,6,14][TFSI] interface, large populations of the cells spread well at the interface (Figure 1f; Figure S15, Supporting Information) at a comparable level to those on glass substrates (**Figure 1g**) with Young's moduli on the order of GPa. The cells on [P4,4,4,1][TFSI] were spread at the interface with a statistically low circularity, while the cell area was not as large as that on [P6,6,6,14][TFSI] (Figure 1h,i). **Figure 2a–h** show the immunofluorescence results of the cytoskeletal structures and focal adhesions (vinculin) of hMSCs adhered to the IL and glass substrate interfaces. As expected from their spherical morphologies (Figure 1d), weak actin stress fibers and poor focal adhesion maturation were observed on [P2,2,2,5][TFSI] as shown in Figure 2a. Whereas for the cells attached at the [P4,4,4,1][TFSI] and [P6,6,6,14][TFSI] interfaces, in similar to the cells at the glass substrate, strong vinculin staining was detected at the edge of *F*-actin, supporting the formation of strong focal adhesions (Figure 2b–h). Among the two well-adhesive ILs, vinculin was mainly located at cellular edges on [P4,4,4,1][TFSI], whereas on [P6,6,6,14][TFSI], it was found throughout the cell basement membrane, suggesting that cells adhered more strongly to the latter interface. Further analysis of cell populations positive for stress fibers and vinculin patches confirmed a gradual increase in cell adhesion strength upon changing the PNLs from [P2,2,2,5][TFSI] to [P6,6,6,14][TFSI] (Figure 2i,j). Moreover, for each IL, we investigated the intracellular distribution of Yes-Associated Protein (YAP) for each IL, whose nuclear localization is increased in cells attached to stiff 2D substrates.[16] In good agreement with the cell morphology results, [P4,4,4,1][TFSI] and [P6,6,6,14][TFSI] showed clear nuclear localization of YAP, whereas [P2,2,2,5][TFSI] did not (Figure 2k–n). Particularly in the case of [P6,6,6,14][TFSI] interface, YAP localization of the nucleus was observed, comparable to that of hMSCs at the glass substrate interface (Figure 2o). This finding indicates that the mechanical properties of the PNL formed at the IL interface vary depending on the chemical structure of the IL.

Given that cell adhesion to the IL interfaces was highly dependent on the IL species, we investigated the PNLs formed at the IL interfaces. In the following study, we characterize PNL at each IL interface using the globular protein bovine serum albumin (BSA). BSA is the main protein component of the culture medium and has been widely studied as a model compound for analyzing the protein adsorption phenomena against various interface.[6,17] Therefore, we decided to use BSA as a suitable model protein for studying biological phenomena in

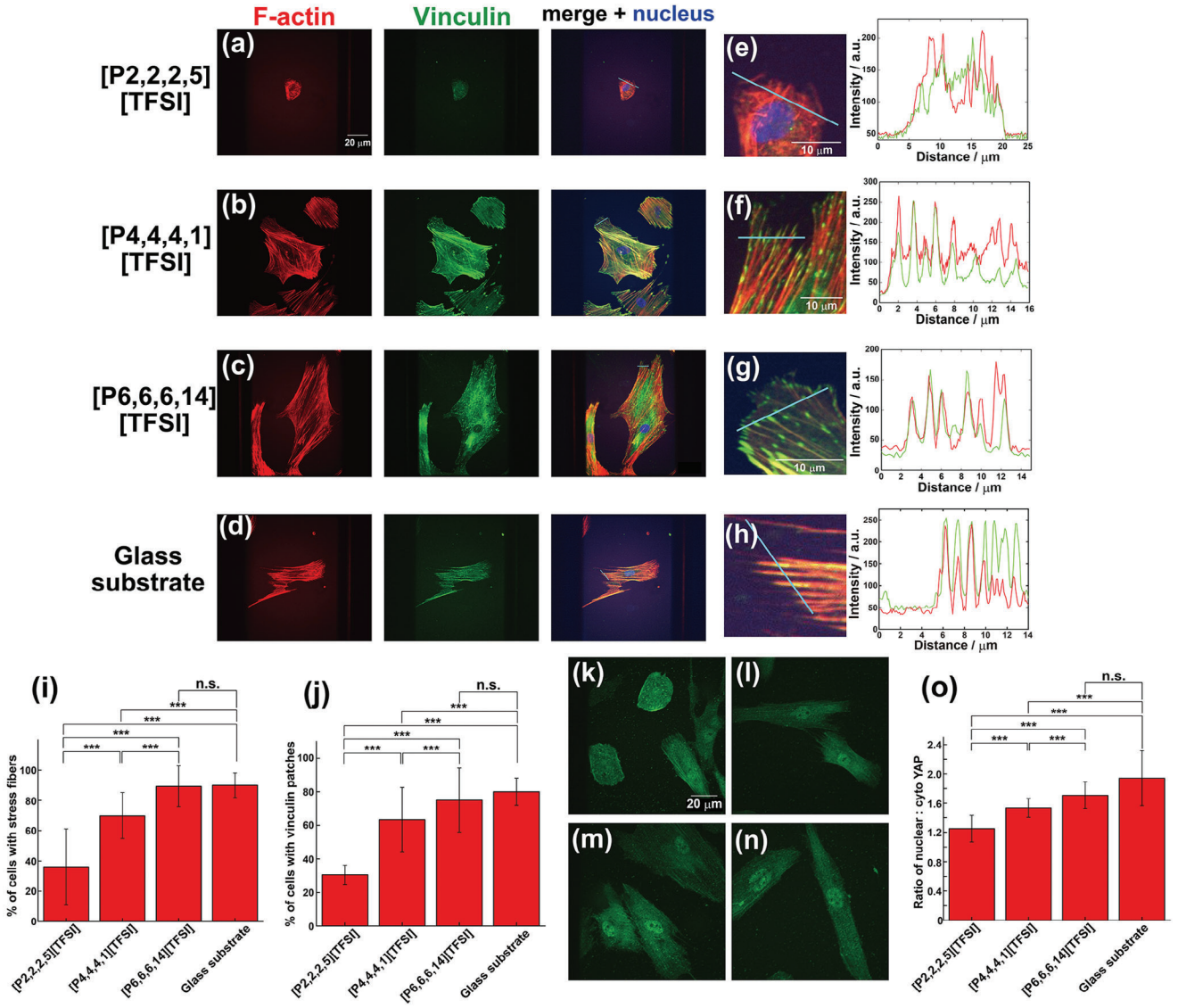

Figure 2. Fluorescence-stained image of *F*-actin (red), vinculin (green), nuclear (blue) of hMSCs cultured at a) [P2,2,2,5][TFSI], b) [P4,4,4,1][TFSI], c) [P6,6,6,14][TFSI], and d) glass substrate for 24 h. Magnified view of merged images e) [P2,2,2,5][TFSI], f) [P4,4,4,1][TFSI], g) [P6,6,6,14][TFSI], and h) glass substrate. Their fluorescence intensity of vinculin and *F*-actin along with the blue line in the photograph is also indicated. i) Percentage of hMSCs with stress fibers and j) the percentage of hMSCs with vinculin patches cultured on [P2,2,2,5][TFSI], [P4,4,4,1][TFSI], [P6,6,6,14][TFSI], and glass substrate interfaces. $n = 36$ ([P2,2,2,5][TFSI]), $n = 30$ ([P4,4,4,1][TFSI]), $n = 28$ ([P6,6,6,14][TFSI]), and $n = 40$ (glass substrate). Fluorescence-stained images of Yes-associated protein (YAP) for k) [P2,2,2,5][TFSI], l) [P4,4,4,1][TFSI], m) [P6,6,6,14][TFSI], and n) glass substrate. o) Quantification of the ratio of nuclear YAP to cytoplasmic YAP for cells cultured on IL interfaces and glass substrate. $n = 13$ ([P2,2,2,5][TFSI]), $n = 11$ ([P4,4,4,1][TFSI]), $n = 12$ ([P6,6,6,14][TFSI]), and $n = 11$ (glass substrate). *** $P < 0.05$ (Student's *t*-test).

unidentified environments, such as ILs interface. Even though the interfacial tension of the three ILs against phosphate buffer saline was significantly lower than that of perfluorocarbons (16–20 vs 53 mN m^{-1}, Figure S16, Supporting Information), apparently similar PNL formation was observed at the interfaces upon the assembly of fluorescence-isothiocyanate (FITC)-labeled BSA as a model protein (Figure S17, Supporting Information). Quantification revealed that the highest BSA adsorption occurred at the [P6,6,6,14][TFSI] interface (Figure S18, Supporting Information); however, the difference was modest compared to the drastic changes in cell morphology (Figures 1,2). Moreover, the fluorescence intensity is greatly affected by the surrounding environment of the fluorophore, thereby it does not represent the amount of the adsorbed protein in a straightforward fashion. Therefore, we analyzed the amount of protein adsorption by ELISA using anti-BSA antibodies (Figure S19, Supporting Information). The results clearly indicated that the amount of adsorbed BSA increased as the subphase IL became less polar. It is reasonable to see stronger protein adsorption observed for the less polar [P6,6,6,14][TFSI] compared to the polar counterparts. Fischer et al. reported the relationship between the subphase hydrophobicity and the stiffness/thickness of the PNLs at the

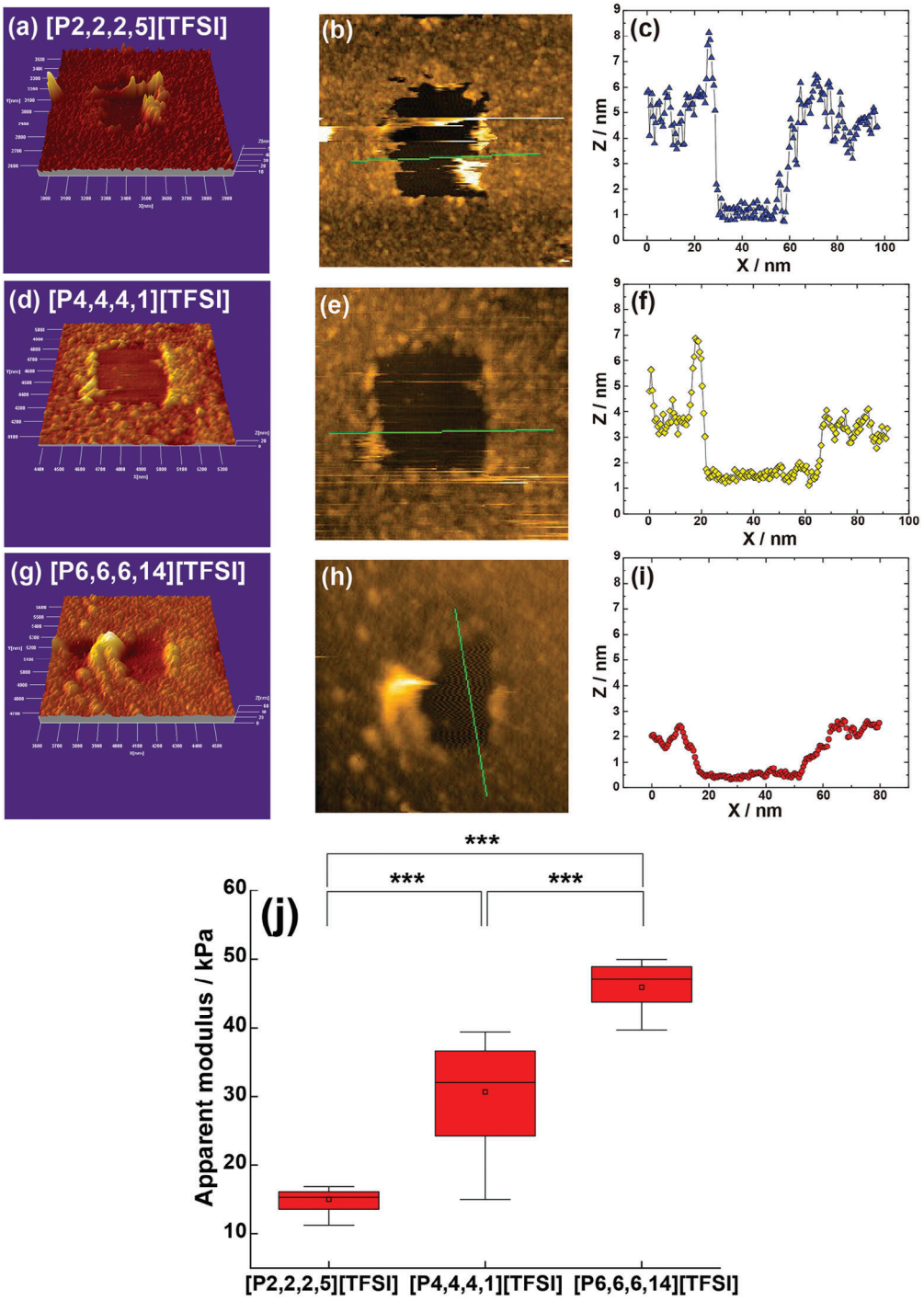

Figure 3. a) A 3D image of PNL formed at [P2,2,2,5][TFSI] interface after scratching by an AFM cantilever, b) an AFM observation image, and c) a height profile. d) A 3D image of PNL formed at [P4,4,4,1][TFSI] interface after scratching by an AFM cantilever, e) an AFM observation image, and f) a height profile. g) A 3D image of PNL formed at [P2,2,2,5][TFSI] interface after scratching by an AFM cantilever, h) an AFM observation image, and i) a height profile. j) Comparison of apparent modulus of PNL formed at IL interfaces measured by nanoindentation. *** $P < 0.05$ (Student's *t*-test).

interface of conventional molecular hydrophobic liquids. Compared to these nonionic hydrophobic liquids, the study of the protein adsorption behaviors to the "ionic" hydrophobic liquids is rare. Therefore, we investigated much more detail in the protein adsorption behaviors to the three ILs, in terms of the thickness and stiffness of PNLs, using in situ liquid AFM observations and nanoindentation.

Figure 3a–i and Figures S20,S21 (Supporting Information) show BSA PNLs covering the three ILs. To estimate the height of the PNLs, they were scratched off by increasing the contact

force between the AFM cantilever and the membrane. The thickness of the PNL gradually decreased from 4 to 1.5 nm by changing the subphase from [P2,2,2,5][TFSI] to [P6,6,6,14][TFSI]. This range corresponds to the short-axis diameter of the BSA molecule (3 nm);[17] therefore it is expected that the PNLs formed at the IL interfaces are composed of monolayer proteins. On the other hand, the AFM nanoindentation analysis of the PNLs showed the apparent moduli of 15.0, 30.6, and 45.9 kPa for [P2,2,2,5][TFSI], [P4,4,4,1][TFSI], and [P6,6,6,14][TFSI], respectively (Figure 3j; Figure S22, Supporting Information).[5a] In this study, we used the Hertz model to roughly estimate the apparent modulus of PNL including other factor than the pure elastic modulus of PNL itself. If accurate mechanical characterization of this system is to be performed, the more sophisticated model should be considered taking into account various effects such as interfacial tension, and adhesion. In addition, Megone et al. recently reported that indentation mechanics is sensitive to various changes at the interface, such as probe-interface interactions.[18] Note that quantitative discussions based on the absolute values of the apparent moduli discussed here may therefore be risky.

PNL nanoindentation was also applied for interfaces that deposited fibronectin, a protein used for conditioning before cell culturing. The apparent moduli of fibronectin PNL were 27.5, 44.8, and 56.2 kPa for [P2,2,2,5][TFSI], [P4,4,4,1][TFSI] and [P6,6,6,14][TFSI], respectively (Figure S23, Supporting Information). The order of stiffness depending on the IL structure was the same as that obtained from BSA. This further indicates possible common trends of the mechanics of PNLs at the IL interfaces. Moreover, the observed inverse relationship between the thickness and mechanical properties was consistent with that reported for PNLs formed at the interface between water and octane derivatives.[6a,c] In that study, Fischer et al. concluded that the polarity of the subphase altered the degree of protein denaturation at the interface, thereby changing the PNLs thicker/thinner and softer/stiffer. By recalling the ELISA results, we could say that more hydrophobic

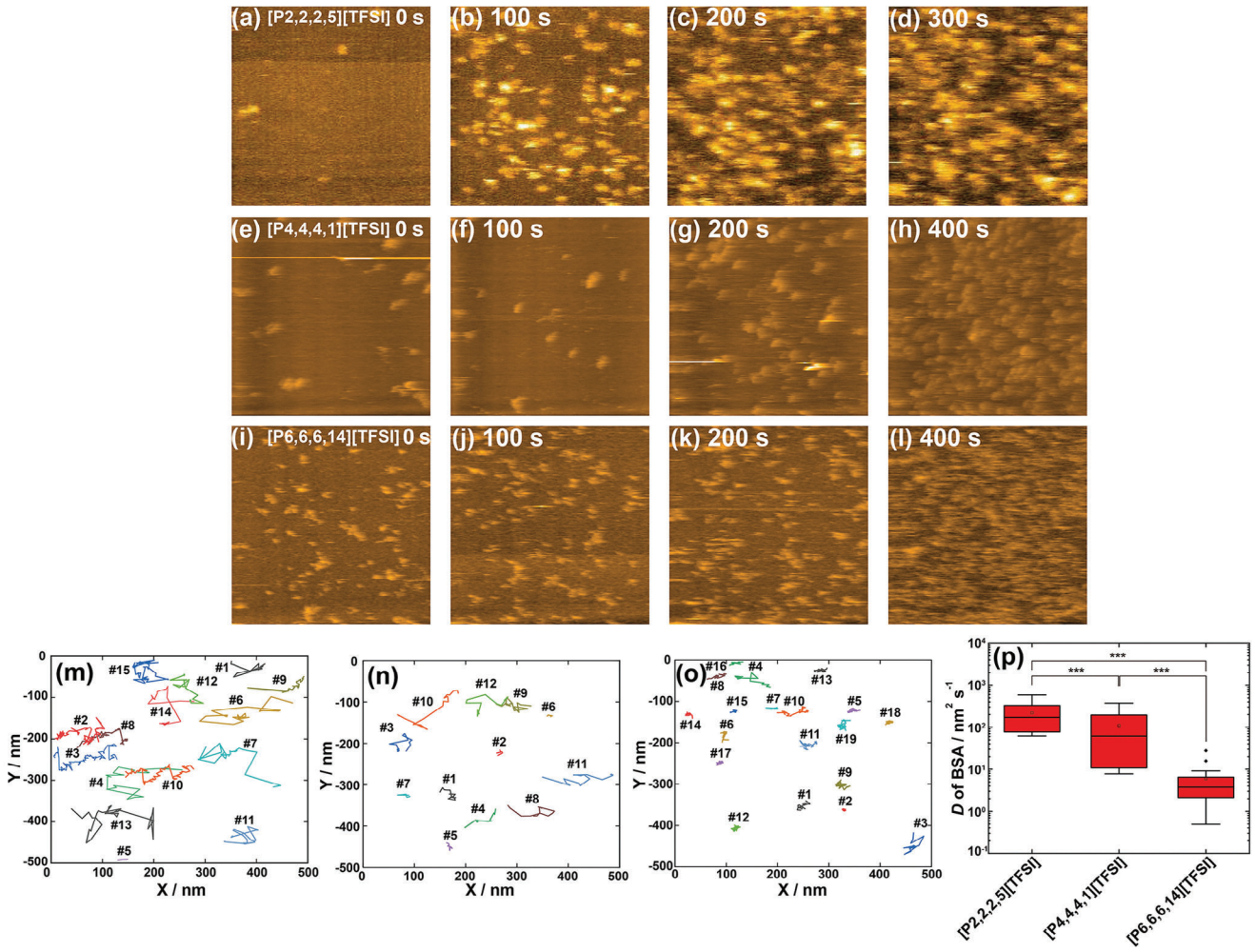

Figure 4. Snapshots of a) 0 s, b) 100 s, c) 200 s, and d) 300 s during the BSA adsorption process on the interface for [P2,2,2,5][TFSI], e) 0 s, f) 100 s, g) 200 s, and h) 400 s for [P4,4,4,1][TFSI], and i) 0 s, j) 100 s, k) 200 s, and l) 400 s for [P6,6,6,14][TFSI]. m) Brownian motion of BSA particle on the surface of [P2,2,2,5][TFSI]. n) Brownian motion of BSA particle on the surface of [P4,4,4,1][TFSI]. o) Brownian motion of BSA particle on the surface of [P6,6,6,14][TFSI]. p) A box plot of the diffusion coefficient of BSA particles at the interface of [P2,2,2,5][TFSI], [P4,4,4,1][TFSI], and [P6,6,6,14][TFSI] estimated from the relationship between the mean square displacement of particles from high-speed AFM and time. *** $P < 0.05$ (Student's *t*-test).

[P6,6,6,14][TFSI] allowed protein adsorption in more denatured structures. Therefore, the amount of protein adsorption as well as the stiffness of the PNLs is supposed to be the major reason for the different cell adhesion behaviors. Furthermore, the FT-IR ATR measurements of PNL formed at the IL interfaces confirmed that the peak intensity ratio of amide I appeared at ≈1650 cm^{-1} and amide II ≈1575 cm^{-1}, a typical indicator of the degree of protein denaturation,[19] increased in the order of [P2,2,2,5][TFSI] < [P4,4,4,1][TFSI] < [P6,6,6,14][TFSI] (Figure S24, Supporting Information). However, the difference in $E_T(30)$ for the three ILs does exist but was by far smaller (47.4 kcal mol^{-1} for [P2,2,2,5][TFSI], 46.6 kcal mol^{-1} for [P4,4,4,1][TFSI], and [P6,6,6,14][TFSI] for 45.5 kcal mol^{-1}) to that discussed in their study (31.1 kcal mol^{-1} for *n*-octane,[20] and 48.1 kcal mol^{-1} for 1-octanol). This indicates unique protein adsorption behaviors at the interfaces of "ionic" "liquids", which differ from those of well-studied ionic crystals,[14] like calcium phosphate, and non-ionic apolar liquids, such as perfluorocarbons and silicones. Thus, the adsorption state (structure and amount) of proteins at the ILs interface is highly dependent on the chemical structure of the ILs themselves. This changes biochemical and mechanical cues exposed to the cells, resulting in different cell adhesion behaviors at the three IL interfaces. Future studies with a wide variety of ILs will be helpful to further optimize PNLs for cell culture scaffolds and to identify dominant factors that regulate protein adsorption behavior at the IL interfaces.

To further address the origin of the different characteristics of PNLs formed at the interfaces of the three ILs, we investigated the dynamic protein adsorption process at molecular resolution using high-speed AFM. Movies S1–S3 (Supporting Information) show the initial stage of BSA adsorption at the [P2,2,2,5][TFSI], [P4,4,4,1][TFSI] and [P6,6,6,14][TFSI] interfaces, respectively. In all ILs, BSA adsorption increased over time and eventually covered the entire surface within 300–500 s. **Figure 4a–l** shows snapshots of the initial adsorption of BSA protein at the interface of the ILs. Interfacial adsorption at the [P6,6,6,14][TFSI] interface started immediately after the earliest stage, whereas BSA adsorption started after an induction period of ≈100 s at the [P2,2,2,5][TFSI], and at the [P4,4,4,1][TFSI] interfaces (Figure S25, Supporting Information). The trajectories of each particle of BSA at the interfaces of [P2,2,2,5][TFSI] (Figure 4m; Figure S26a, Supporting Information) exhibit a large displacement, whereas [P6,6,6,14][TFSI] (Figure 4o; Figure S26c, Supporting Information) exhibit a small displacement. In contrast to these two extreme cases, BSA on [P4,4,4,1][TFSI] appears to have a small number of stagnant species mixed in with most particles moving around frequently (Figure 4n; Figure S26b, Supporting Information). The 2D diffusion coefficient (*D*) of BSA at [P2,2,2,5][TFSI], [P4,4,4,1][TFSI] and [P6,6,6,14][TFSI] interfaces were 1.71×10^{-10} (cm^2 s^{-1}), 6.18×10^{-11} (cm^2 s^{-1}) and 3.73×10^{-12} (cm^2 s^{-1}), respectively (Figure 4p), with approximately two orders difference among them. This indicated a stronger protein interaction with the [P6,6,6,14][TFSI] interface. At the [P6,6,6,14][TFSI] interface, BSA denatures immediatery at the liquid interface and is adsorbed with hydrophobic interaction when the protein comes into contact with the interface. This attractive interaction acts as a resistance against diffusion on the protein particles, which suppresses Brownian motion. In contrast, in [P2,2,2,5][TFSI] or [P4,4,4,1][TFSI], BSA frequently moves across the interface, diffuses and is gradually adsorbed; hence, such a resistance against diffusion does not work effectively, resulting in a higher *D* than that at the [P6,6,6,14][TFSI] interface. This diffusion behavior of BSA at each IL interface may be partially affected by the orientational direction of cations at the IL | water interface reflecting

Table 1. Summary of solubility tests for poly(meth)acrylates, polystyrenes, and polyacrylamides toward [P2,2,2,5][TFSI], [P4,4,4,1][TFSI], and [P6,6,6,14][TFSI] as a solvent. Each polymer (2 wt.%) is mixed with ILs by the co-solvent evaporation method. Transparency was judged by the naked eyes. Yes: Transparent, homogeneous mixture with a range from 4 to 100 °C. No: Turbid phase separation within a range from 4 to 100 °C.

	1. PMMA	2. PEMA	3. P(*iso*-Pro)MA	4. P(*n*-Bu)MA	5. P(*iso*-Bu)MA	6. P(*n*-Hex)MA	7. P(*c*-Hex)MA
[P2,2,2,5][TFSI]	Yes	Yes	Yes	Yes	Yes	No	No
[P4,4,4,1][TFSI]	Yes	Yes	Yes	Yes	Yes	No	No
[P6,6,6,14][TFSI]	Yes	Yes	Yes	Yes	Yes	No	No

	8. P(*n*-Dod)MA	9. PBnMA	10. PMA	11. PEA	12. P(*iso*-Pro)A	13. P(*n*-Bu)A	14. P(*iso*-Bu)A
[P2,2,2,5][TFSI]	No	No	Yes	Yes	Yes	Yes	Yes
[P4,4,4,1][TFSI]	No	No	Yes	Yes	Yes	Yes	Yes
[P6,6,6,14][TFSI]	No	No	Yes	Yes	Yes	Yes	Yes

	15. P(*n*-Hex)A	16. P(*n*-Dec)A	17. P(*n*-Dod)A	18. PSt	19. P(*α*-Me)St	20. PVnTol	21. P(*tert*-Bu)St
[P2,2,2,5][TFSI]	No	No	No	No	No	No	No
[P4,4,4,1][TFSI]	No	No	No	No	No	No	No
[P6,6,6,14][TFSI]	No	No	No	No	No	No	No

	22. PVnBn-Cl	23. P(*tri*-Br)St	24. PAAm	25. PDMAm	26. PDEAm	27. PNIPAm	28. PACMO
[P2,2,2,5][TFSI]	No	No	No	Yes	Yes	UCST(40–50 °C)	No
[P4,4,4,1][TFSI]	No	No	No	Yes	Yes	UCST(50–60 °C)	No
[P6,6,6,14][TFSI]	No	No	No	No	Yes	No	No

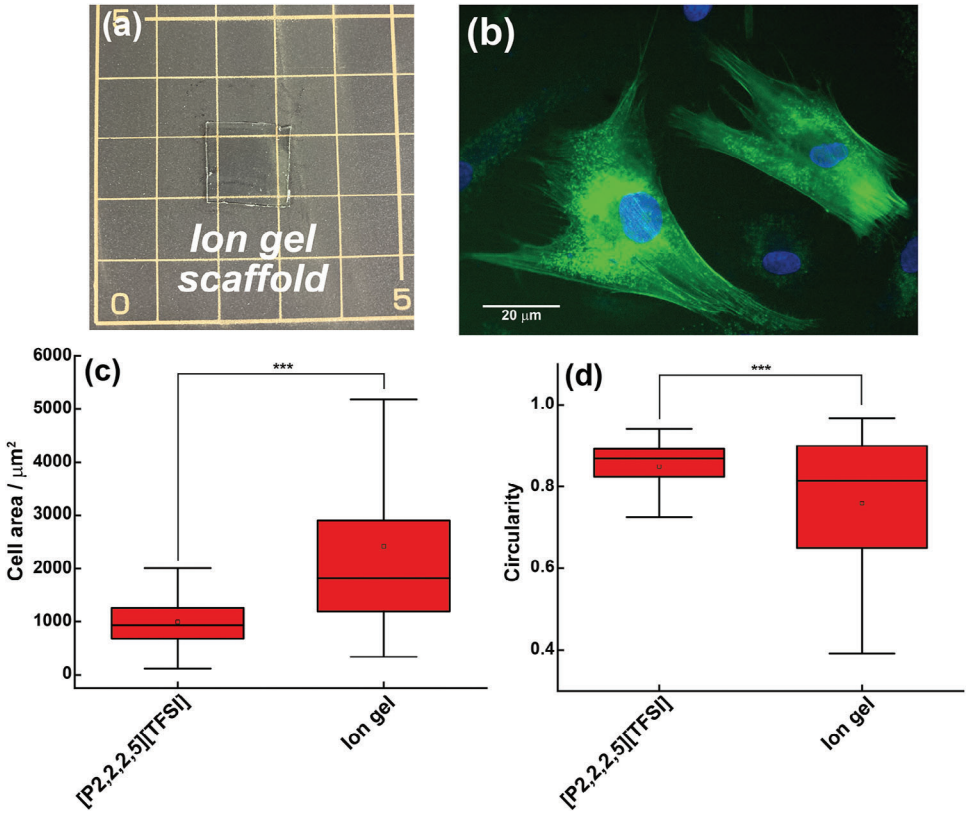

Figure 5. a) A photograph of an ion gel obtained by in situ radical polymerization of *n*-butylmethacrylate (*n*BuMA) as a monomer, ethylene glycol dimethacrylate (EGDMA) as a cross-linker and azobis(isobutyronitrile) (AIBN) as an initiator in [P2,2,2,5][TFSI] as a solvent. The contents of the pre-gel solution are as follows: [*n*-BuMA] = 2 M, [EGDMA] = 5 mol% versus *n*-BuMA, and [AIBN] = 1 mol% versus *n*-BuMA. b) Fluorescence microscopic observation of hMSCs transiently expressing LifeAct-GFP attached hMSCs at the interface of a [P2,2,2,5][TFSI] ion gel. Comparison of the c) cell area and d) circularity of hMSCs cultured at [P2,2,2,5][TFSI] liquid interface and [P2,2,2,5][TFSI]-P*n*BuMA ion gel. *** $P < 0.05$ (Student's *t*-test).

interfacial tension.[21] The difference in membrane mechanics is likely attributed to the interfacial phenomena of the initial adsorption process rather than bulk polarity such as $E_T(30)$. We have tried to observe the BSA adsorption process at the interface of perfluorooctane (PFO) which is used for liquid cell culture, as a control. However, the adsorption process of BSA was completed too quickly to be monitored by high-speed AFM. It is noteworthy that protein adsorption dynamics bacame detactable speed and manipulatable only when we use ILs as the subphase. Note that zwitterionic materials, such as poly(2-methacryloyloxyethyl phosphorylcholine) (PMPC),[22] and polysulfobetaines (PSB),[23] are resistant against protein adsorption due to two closely charged cations and anions. The major expected differences among the ILs tested in this study are ion-pairing depending on the length of the alkyl chains conjugated to the phosphonium cations; therefore, it is reasonable to observe different protein adsorption behaviors. Further systematic studies are needed to understand the relationship between protein adsorption kinetics and the mechanical maturation of the PNLs on ILs and are underway to take advantage of the designers' nature of ILs. High-speed AFM observations also suggested that the PNL was formed as a monolayer and exhibited self-healing properties (Movies S4,S5, Supporting Information). This suggests that an IL interface can be used for the 2D protein concentration process without significant conformational changes in the tertiary structure of the protein.[6c]

Finally, we developed the unique capacity of the IL-based scaffolds to manipulate the physicochemical properties of the liquid phases. The fracturing of PNLs by an accidental mechanical perturbation is supposed to be one disadvantage of liquid-based scaffolds. The conventional perfluorocarbon- and silicone-based scaffolds can only be reinforced by engineering PNLs, either by crosslinking with perfluorobenzoyl chloride,[2b,c,3a,24] or depositing denatured protein.[25] Unlike fluorocarbons, which are poor solvents for conventional polymers (Table S2, Supporting Information), ILs can dissolve various conventional polymers;[10b,c] therefore, we were able to manipulate the mechanical properties of the liquid bulk (**Table 1**, Figure S27, Supporting Information). Here, we transformed the IL [P2,2,2,5][TFSI] into a free-standing "ion gel" by in situ radical polymerization of *n*-(butyl methacrylate) (*n*BuMA) monomer in the presence of bifunctional ethylene glycol dimethacrylate (EGDMA) (**Figure 5a**; Figure S28, Supporting Information). Figure 5b shows the adhesion morphology of hMSCs attached to the interface [P2,2,2,5][TFSI] ion gel. In sharp contrast to the poorly adhesive nature of the original [P2,2,2,5][TFSI] (Figure 1d,h,i), hMSCs exhibit spreading morphology with enhanced spreading area and lower circularity, indicating improved adhesion on the [P2,2,2,5][TFSI] ion gel (Figure 5c,d). Since both the IL and the [P2,2,2,5][TFSI] ion gel were subjected to the same interface modification treatment, the difference in cell adhesion reflects the bulk properties of the

substrate. In other words, the mechanically less robust PNLs formed at the [P2,2,2,5][TFSI] interface were complemented by the bulk mechanics of the ion gels to support cell adhesion. This feature will be useful not only for decoupling the contribution of the interface and bulk properties to cell adhesion behaviors from the mechanobiology viewpoints but also for endowing the liquid phase with a stimulus-responsive nature (See, UCST behaviors of poly(*N*-isopropylacrylamide (PNIPAm) in Table 1), which highlights high-polar but water-immiscible ion gel as a versatile platforms for cell cultures. Studies on the changes in cellular behavior on mechanical property controllable ion gels are currently in progress and will be reported elsewhere in the future.

3. Conclusion

We described the culture of cells at the IL interface. Although hydrophobic ILs do not mix with water because ILs are composed only of ions, they provide an interface that differs from that of fluorocarbons, a common liquid-cell culturing scaffold. Emulsion culturing using a hydrophobic liquid as the dispersed phase and a cell culture medium as the continuous phase has been proposed as a promising developmental application of cell culturing at the liquid interface.[2b,3,26] If this culturing technology can be established, its culturing efficiency can be remarkably enhanced compared to the conventional 2D culture method using plastic dishes. By exploiting the deformability of liquids, it is possible to recover cell resources through a filtration process that does not require trypsin enzyme treatment, thereby facilitating full automation of the cell culture process. If the nonflammable and nonvolatile "green" hydrophobic ILs can be utilized for this purpose, water washable (recyclable) and dry-heat-sterilized available dispersion phase will be realized. Currently, in addition to gaining deep insight into the basic science of cell culturing at the interface of ILs, studies on emulsion cell culturing using ILs are ongoing.

Supporting Information

Supporting Information is available from the Wiley Online Library or from the author.

Acknowledgements

This study was financially supported by JSPS KAKENHI grants (20H02804, 20K21229, and 23H02030 to T. U., 22K14705 to S. Y., and 22H00596, and 23K17481 to J. N.). The authors thank the Research Institute of Biomolecule Metrology (RIBM) Co. Ltd. for direct observation of PNL using high-speed AFM. T.U. greatly thanks to Naoya Nishi for fruitful discussions on the orientation of ILs at the water interface. T.U. and J.N. also thank Mayumi Takenouchi, and Kaho Nomura for their helpful assistance for the experiment.

Conflict of Interest

The authors declare no conflict of interest.

Data Availability Statement

The data that support the findings of this study are available from the corresponding author upon reasonable request.

Keywords

cell cultures, gels, ionic liquids, liquid interface, mechanobiology

Received: September 29, 2023
Revised: January 7, 2024
Published online:

[1] a) D. E. Ingber, *Ann. Med.* **2003**, *35*, 564; b) D. H. Kim, P. K. Wong, J. Park, A. Levchenko, Y. Sun, *Annu. Rev. Biomed. Eng.* **2009**, *11*, 203; c) T. Mammoto, A. Mammoto, D. E. Ingber, *Annu. Rev. Cell Dev. Biol.* **2013**, *29*, 27.
[2] a) M. D. Rosenberg, *Cell surface interactions and interfacial dynamics*, Elsevier, Amsterdam, Netherlands **1964**; b) I. Giaever, C. R. Keese, *Proc. Natl. Acad. Sci. U. S. A.* **1983**, *80*, 219; c) C. R. Keese, I. Giaever, *Proc. Natl. Acad. Sci. U. S. A.* **1983**, *80*, 5622; d) C. R. Keese, I. Giaever, *Science* **1983**, *219*, 1448.
[3] a) D. Kong, L. Peng, S. Di Cio, P. Novak, J. E. Gautrot, *ACS Nano* **2018**, *12*, 9206; b) L. Peng, J. E. Gautrot, *Mater Today Bio* **2021**, *12*, 100159.
[4] a) K. Minami, T. Mori, W. Nakanishi, N. Shigi, J. Nakanishi, J. P. Hill, M. Komiyama, K. Ariga, *ACS Appl. Mater. Interfaces* **2017**, *9*, 30553; b) X. F. Jia, K. Minami, K. Uto, A. C. Chang, J. P. Hill, T. Ueki, J. Nakanishi, K. Ariga, *Small* **2019**, *15*, 1804640; c) D. Kong, K. D. Q. Nguyen, W. Megone, L. Peng, J. E. Gautrot, *Faraday Discuss.* **2017**, *204*, 367; d) D. Kong, W. Megone, K. D. Q. Nguyen, S. Di Cio, M. Ramstedt, J. E. Gautrot, *Nano Lett* **2018**, *18*, 1946.
[5] a) X. Jia, K. Minami, K. Uto, A. C. Chang, J. P. Hill, J. Nakanishi, K. Ariga, *Adv. Mater.* **2020**, *32*, 1905942; b) X. Jia, J. Song, W. Lv, J. P. Hill, J. Nakanishi, K. Ariga, *Nat. Commun.* **2022**, *13*, 3110; c) W. Lyu, W. Hu, J. Shi, J. Chen, J. Song, Q. Zhang, X. Yuan, D. Li, J. Nakanishi, X. Jia, *Adv. Healthcare Mater.* **2023**, *12*, 2300666.
[6] a) J. Bergfreund, P. Bertsch, P. Fischer, *J. Colloid Interface Sci.* **2021**, *584*, 411; b) J. Bergfreund, P. Bertsch, P. Fischer, *Curr. Opin. Colloid Interface Sci.* **2021**, 56; c) J. Bergfreund, M. Diener, T. Geue, N. Nussbaum, N. Kummer, P. Bertsch, G. Nystrom, P. Fischer, *Soft Matter* **2021**, *17*, 1692.
[7] M. S. Rudnicki, H. A. Cirka, M. Aghvami, E. A. Sander, Q. Wen, K. L. Billiar, *Biophys. J.* **2013**, *105*, 11.
[8] *Ionic liquids 3A; Fundamentals, Progress, Challenges, and Opportunities Properties and Structure*, (Ed.: R. D. Rogers, K. R. Seddon), American Chemical Society Symposium Series, Washington D. C **2005**.
[9] a) T. Welton, *Chem. Rev.* **1999**, *99*, 2071; b) M. J. Earle, K. R. Seddon, *Pure Appl. Chem.* **2000**, *72*, 1391; c) N. V. Plechkova, K. R. Seddon, *Chem. Soc. Rev.* **2008**, *37*, 123.
[10] a) A. Arce, M. J. Earle, S. P. Katdare, H. Rodriguez, K. R. Seddon, *Chem. Commun.* **2006**, 2548; b) N. Winterton, *J. Mater. Chem.* **2006**, *16*, 4281; c) T. Ueki, M. Watanabe, *Bull. Chem. Soc. Jpn.* **2012**, *85*, 33.
[11] a) T. Ueki, M. Watanabe, *Macromolecules* **2008**, *41*, 3739; b) R. Tamate, T. Ueki, *Chem. Rec.* **2023**, *23*, 202300043.
[12] K. J. Fraser, E. I. Izgorodina, M. Forsyth, J. L. Scott, D. R. MacFarlane, *Chem. Commun.* **2007**, 3817.
[13] K. Ueno, H. Tokuda, M. Watanabe, *Phys. Chem. Chem. Phys.* **2010**, *12*, 1649.
[14] K. Wang, M. Wang, Q. Wang, X. Lu, X. Zhang, *J. Eur. Ceram. Soc.* **2017**, *37*, 2509.
[15] a) C. Reichardt, *Green Chem.* **2005**, *7*, 339; b) Y. Marcus, *West Sussex PO19 1UD*, John Wiley & Sons Ltd, England **1998**.
[16] S. Dupont, L. Morsut, M. Aragona, E. Enzo, S. Giulitti, M. Cordenonsi, F. Zanconato, J. L. Digabel, M. Forcato, S. Bicciato, N. Elvassore, S. Piccolo, *Nature* **2011**, *474*, 179.
[17] Y. F. Yano, *J. Phys. Condens. Matter* **2012**, *24*, 503101.

[18] W. Megone, D. Kong, L. Peng, J. E. Gautrot, *J. Colloid Interface Sci.* **2021**, *594*, 650.
[19] a) P. Roach, D. Farrar, C. C. Perry, *J. Am. Chem. Soc.* **2005**, *127*, 8168; b) P. Roach, D. Farrar, C. C. Perry, *J. Am. Chem. Soc.* **2006**, *128*, 3939.
[20] C. Reichardt, *Chem. Rev.* **1994**, *94*, 2319.
[21] K. Ishii, T. Sakka, N. Nishi, *Phys. Chem. Chem. Phys.* **2021**, *23*, 22367.
[22] Y. Iwasaki, K. Ishihara, *Sci. Technol. Adv. Mater.* **2012**, *13*, 064101.
[23] S. Jiang, Z. Cao, *Adv. Mater.* **2010**, *22*, 920.
[24] a) L. Wu, S. Di Cio, H. S. Azevedo, J. E. Gautrot, *Biomacromolecules* **2020**, *21*, 4663; b) C. R. Keese, I. Giaever, *Exp. Cell Res.* **1991**, *195*, 528.
[25] a) Y. Shiba, T. Ohshima, M. Sato, *Biotechnol. Bioeng.* **1998**, *57*, 583; b) Y. Shiba, T. Ohshima, M. Sato, *Kagaku Kogaku Ronbunshu* **1998**, *24*, 343.
[26] D. Kong, L. Peng, M. Bosch-Fortea, A. Chrysanthou, C. V. J. Alexis, C. Matellan, A. Zarbakhsh, G. Mastroianni, A. Del Rio Hernandez, J. E. Gautrot, *Biomaterials* **2022**, *284*, 121494.